Certification of Genuine Multipartite Entanglement with General and Robust Device-Independent Witnesses

Chao Zhang,[1,2,3] Wen-Hao Zhang,[1,2,3] Pavel Sekatski,[4,*] Jean-Daniel Bancal,[5,†] Michael Zwerger,[6,‡] Peng Yin,[1,2,3] Gong-Chu Li,[1,2,3] Xing-Xiang Peng,[1,2,3] Lei Chen,[1,2,3] Yong-Jian Han,[1,2,3] Jin-Shi Xu,[1,2,3] Yun-Feng Huang,[1,2,3,§] Geng Chen,[1,2,3,‖] Chuan-Feng Li,[1,2,3,¶] and Guang-Can Guo[1,2,3]

[1]*CAS Key Laboratory of Quantum Information, University of Science and Technology of China, Hefei, Anhui 230026, China*
[2]*CAS Center For Excellence in Quantum Information and Quantum Physics, University of Science and Technology of China, Hefei, Anhui 230026, China*
[3]*Hefei National Laboratory, University of Science and Technology of China, Hefei 230088, China*
[4]*Department of Applied Physics, University of Geneva, Rue de l'École-de-Médecine, 1211 Geneva, Switzerland*
[5]*Université Paris-Saclay, CEA, CNRS, Institut de physique théorique, 91191 Gif-sur-Yvette, France*
[6]*Max Planck Institute for the Science of Light, Erlangen 91058, Germany*

(Received 4 November 2021; accepted 28 September 2022; published 31 October 2022)

Genuine multipartite entanglement represents the strongest type of entanglement, which is an essential resource for quantum information processing. Standard methods to detect genuine multipartite entanglement, e.g., entanglement witnesses, state tomography, or quantum state verification, require full knowledge of the Hilbert space dimension and precise calibration of measurement devices, which are usually difficult to acquire in an experiment. The most radical way to overcome these problems is to detect entanglement solely based on the Bell-like correlations of measurement outcomes collected in the experiment, namely, device independently. However, it is difficult to certify genuine entanglement of practical multipartite states in this way, and even more difficult to quantify it, due to the difficulty in identifying optimal multipartite Bell inequalities and protocols tolerant to state impurity. In this Letter, we explore a general and robust device-independent method that can be applied to various realistic multipartite quantum states in arbitrary finite dimension, while merely relying on bipartite Bell inequalities. Our method allows us both to certify the presence of genuine multipartite entanglement and to quantify it. Several important classes of entangled states are tested with this method, leading to the detection of genuinely entangled states. We also certify genuine multipartite entanglement in weakly entangled Greenberger-Horne-Zeilinger states, showing that the method applies equally well to less standard states.

DOI: 10.1103/PhysRevLett.129.190503

Introduction.—Genuine multipartite entanglement (GME) is a topic of intense research because of its importance in quantum computation and condensed matter physics. Currently available techniques have realized Schrödinger cat states of up to 20 qubits [1,2]. A natural question arising in such experiments is how to certify the presence of GME. Usual solutions consist of measuring a witness [3–5] of GME, doing a full state tomography and analyzing the reconstructed density matrix [6–8], or executing quantum state verification on the premise of accessing some partial prior knowledge about the state [9–12]. These approaches require sufficient knowledge of the internal physics of the measurement devices and the dimension for the Hilbert space of each system [13]. Unfortunately, it is usually difficult to access an exact quantum description of measurement devices; moreover, the actual measurement settings may deviate from the expected ones slightly and result in an incorrect conclusion [14]. Furthermore, a physical system typically has access to more levels and degrees of freedom than one uses to describe its state. In fact, using an inappropriate description of the system at hand can have devastating consequences when using it for quantum applications, as demonstrated in recent hacking experiments [15,16].

In order to circumvent this problem, researchers opened a new realm of quantum science, namely "device-independent" science [17–26], in which no assumptions are made about the states under observation, the experimental measurement devices, or even the dimensionality of the Hilbert spaces where such elements are defined. In this approach, the only way to study a system is to perform local measurements on well-separated subsystems and analyze the statistical results. Many theoretical and experimental efforts have been devoted to device-independent certification (DIC) of bipartite entangled states based on Bell tests [27–30]. But it is still a formidable challenge to extend this method to general multipartite scenarios. The difficulty mainly results from the lack of multipartite Bell inequalities tailored to arbitrary quantum states. Furthermore, for the known inequalities the complexity (number of different measurements to perform) typically increases exponentially with the number of parties,

making them impractical. To date, DIC has been intensively investigated for a few simple types of multipartite entangled states [31–34], and several specific genuinely entangled states [35–38] have been investigated. Similarly, self-testing, an approach allowing one to identify the quantum state device independently was only pursued for a few states [39–44]. Recently, a dissociated DIC (DDIC) method to detect GME was proposed, whereby the detection of GME is reduced into a set of bipartite problems, for each of which a bipartite Bell inequality is tested [45]. For multiqubit states it is sufficient to use the tilted Clauser-Horne-Shimony-Holt (CHSH) family of Bell tests [46], while in general one can rely on the results of [41], which allow one to self-test arbitrary pure bipartite states in finite dimension. This scheme applies to all multipartite pure states in arbitrary finite dimension and tolerates nonmaximal violation; however, the level of admissible noise is limited.

In this Letter, we build on the technique of [45] and generalize the DDIC method to improve its robustness to noise. We investigate different covering sets of the DDIC method and find that the full covering is more tolerant to noise. We further show the biseparable bound for the full covering is both optimal and tight. The overhead of the scheme does not scale exponentially with the system size, which makes it suitable in practice. Using the polarization of single photons, we test several essential entangled states experimentally, including Greenberger-Horne-Zeilinger (GHZ) states, partially entangled states, and cluster states.

The limited detection efficiency in our experiment leads to the occurrence of no-click events. Simply rejecting these events (postselection) opens the infamous detection loophole, and forbids the device-independent analysis of the postselected measurement data. This problem is overcome here by introducing a minimal assumption on the internal functioning of the measurement devices, the so-called weak fair-sampling assumption [47], which is well justified in our setup.

Device independent certification of GME.—The main target of this Letter is to distinguish genuinely entangled states from biseparable ones, which can be expressed as

$$\rho_{BS} = \sum_{g_1,g_2} P_{g_1|g_2} \sum_{\lambda} P(\lambda) \rho_{g_1}(\lambda) \otimes \rho_{g_2}(\lambda), \qquad (1)$$

where the groups $g_1 \cup g_2 = \{1, \ldots, N\}$ form a bipartition of the N parties, the first sum runs over all such splittings, ρ_{g_1} and ρ_{g_2} are arbitrary quantum states of the parties belonging to the respective group, and λ is a variable distributed accordingly to $P(\lambda)$. By definition, genuinely multipartite entangled states (GME states) cannot be written in this form, and involve a contribution that does not split as a tensor product for any bipartition. To illustrate this phenomenon, Fig. 1(a) shows a graph representation of the decomposition for $N = 4$. The state is GME if and only if the lowest possible value of P_{ABCD} in the decomposition is larger than zero. We now only consider decompositions where P_{ABCD} is minimal.

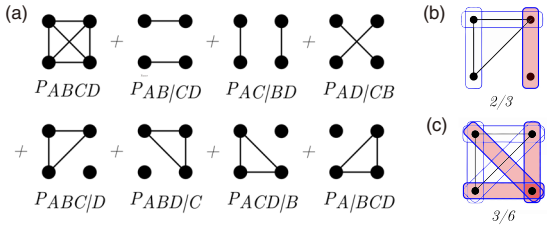

FIG. 1. Graph representation of multipartite states. (a) Graphical representation of a general decomposition of a four-partite state into a mixture of a GME state and biseparable states in the respective bipartition. Here, each vertex corresponds to a party, and connected parties belonging to the same group. (b) A linear minimum covering (blue boxes) of a four-partite state, only one link (pink filled) is cut by the bipartition $\rho_{ABC|D}$. (c) A full covering of a four-partite state, half of the edges are cut by the bipartition $\rho_{ABC|D}$.

A GME state can be device-independently certified as we will now show; the three steps of our protocol are summarized in the Supplemental Material (SM) [48]. To start, we chose a covering E—a set of pairs of parties (edges) defining a graph connecting all parties. Then, we aim to reveal bipartite Bell nonlocality for each edge $e = \{i, j\} \in E$. To achieve this, the remaining parties in $R \subset \{1, \ldots, N\} \backslash e$ are first measured in order to leave the parties e in a pure entangled state [53]. For each branch, defined by the combination of measurement outcomes on R, we test some bipartite Bell inequality between the parties in e with fixed local bound β^L and quantum bound $\beta^Q > \beta^L$. The Bell score β_e associated to the edge e is then defined as the average of the Bell scores obtained over all branches. In the ideal case, all the Bell tests can be chosen such that $\beta_e = \beta^Q$. Finally, the observation of a large enough average score $\bar{\beta}^E = (1/|E|) \sum_{e \in E} \beta_e$ over all pairs $e \in E$ allows one to infer that the underlying state is GME [45].

Indeed, if the measured state can be decomposed in the form of Eq. (1) (with $P_{ABCD} = 0$ in the example), each term $\rho_{g_1} \otimes \rho_{g_2}$ in the decomposition "cuts" at least one edge $e \in E$. More precisely, there is at least one pair $e = \{i, j\}$ with the two parties belonging to different groups $i \in g_1$ and $j \in g_2$. For this term the Bell score β_e cannot exceed the local bound $\beta^L < \beta^Q$. As this happens for each term, the biseparable bound is necessarily lower than the quantum maximum $\bar{\beta}^E_{\mathrm{BS}} < \beta^Q$, and observing a value $\bar{\beta}^E$ exceeding $\bar{\beta}^E_{\mathrm{BS}}$ proves GME. Moreover, the fact that this inequality is strict implies that the test admits some robustness to noise. However, the precise value of this biseparable bound depends on the chosen covering E.

To see this, consider two extreme cases of coverings: the minimal covering E_{mini} with $|E_{\mathrm{mini}}| = N - 1$ edges (minimally connected graph) and the full covering E_{full} with $|E_{\mathrm{full}}| = N(N-1)/2$ edges (fully connected graph). In the case of minimal covering, one can always find a bipartition that only cuts one edge; see Fig. 1(b). Therefore, for E_{mini}

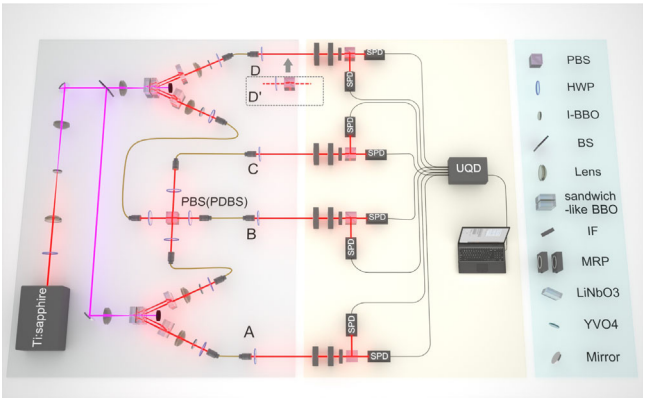

FIG. 2. Experimental setup. A frequency-doubled mode-locked Ti:sapphire laser (390 nm, 140 fs, and 80 MHz) is split averagely into two beams and used to pump two sandwichlike EPR sources (see SM [48] for details). Two photons (each from a source) are overlapped on the central polarization beam splitter (PBS)/polarization-dependent beam splitter (PDBS) to generate different class of four-photon entangled state. To generate biseparable state, a HWP and a PBS is inserted in photon D. The Bell correlation is measured through four sets of polarization analyzer setup (PAS). Each PAS consists of elements rotating the polarization of incident photons in a controlled way, followed by a PBS and two single photon detectors (SPD). Symbols are HWP, half-wave plate; IF, interference filter; MRP, motorized rotation plate. The PAS satisfies the weak-fair sampling assumption as discussed in SM [48].

the biseparable bound on the average Bell score is given by $\bar{\beta}^{\text{mini}}_{\text{BS}} = \{[(|E_{\text{mini}}|-1)\beta^Q+\beta^L]/(|E_{\text{mini}}|)\} = \beta^Q - [(\beta^Q-\beta^L)/(N-1)]$. In the case of a full covering any bipartition cuts at least $N-1$ edges; see Fig. 1(c). Normalizing by the number of pairs the biseparable bound for a full covering reads $\bar{\beta}^{\text{full}}_{\text{BS}} = (\{[|E_{\text{full}}|-(N-1)]\beta^Q+(N-1)\beta^L\}/|E_{\text{full}}|) = \beta^Q - 2[(\beta^Q-\beta^L)/N]$. It can be easily seen that $\bar{\beta}^{\text{full}}_{\text{BS}}$ is lower than $\bar{\beta}^{\text{mini}}_{\text{BS}}$, which is a natural since measuring more edges reveals more information about the structure of the state, helping to certify GME. Hence, the full covering is more tolerant to noise. In SM [48] we show that the biseparable bound for the full covering is optimal, as one naturally expects, i.e., there is no covering E for which a lower average violation $\bar{\beta}^E \leq \bar{\beta}^{\text{full}}_{\text{BS}}$ certifies GME.

Note that these required violations $\bar{\beta}^{\text{full}}_{\text{BS}}$ and $\bar{\beta}^{\text{mini}}_{\text{BS}}$ are strictly larger than the local bound β^L, as one would expect. Indeed, biseparable states can be mixtures of states that are separable according to different partitions, and can therefore produce some Bell violation for each pair of parties. In SM [48], we construct a class of biseparable states that saturate the bounds $\bar{\beta}^{\text{full}}_{\text{BS}}$ and $\bar{\beta}^{\text{mini}}_{\text{BS}}$ and thus demonstrate they are tight.

Whereas the full covering comes with a higher noise tolerance it also makes the protocol less practical. Indeed, the number of pairs in the covering become quadratic in N instead of linear. Clearly, the minimal and full covering are the two limiting cases. Interestingly, we show in SM [48] that a ring covering E_{ring} also saturates the optimal biseparable bound $\bar{\beta}^{\text{ring}}_{\text{BS}} = \bar{\beta}^{\text{full}}_{\text{BS}}$, while only involving a linear number of edges $|E_{\text{ring}}| = N$. The number of parties that have to be measured in order to prepare an entangled state between some pair e appearing in the covering also scales with the system size in general. For practical purposes it is helpful if entangled states can be prepared by operating on a small number of parties for all pairs added to the covering. This can be done generically for interesting states, such as generalized, weighted graph states with bounded degree.

It is worth noting, however, that all states' preparations need not be evaluated in practice in order to conclude about GME: since every such preparation across a biseparation must satisfy the local bound, finding one violation is enough to conclude about GME. In other words, a statistically significant violation of our witness over one edge e can be concluded after a number of samplings that is fixed, i.e., that does not scale with N.

DDIC method as a measure of GME.—For any multipartite quantum state ρ, let

$$\rho = P_{\text{GME}}\rho_{\text{GME}} + P_{\text{BS}}\rho_{\text{BS}} \tag{2}$$

with ρ_{BS} biseparable as the decomposition that maximizes the biseparable weight $P_{\text{BS}} = 1 - P_{\text{GME}}$. For such state the DDIC score cannot exceed $\bar{\beta}^E \leq P_{\text{GME}}\beta_Q + P_{\text{BS}}\bar{\beta}^E_{\text{BS}}$ by linearity. Thus, the observation of a value for $\bar{\beta}_E$ sets a lower bound,

$$P_{\text{GME}} \geq \frac{\bar{\beta}^E - \bar{\beta}^E_{\text{BS}}}{\beta_Q - \bar{\beta}^E_{\text{BS}}}, \tag{3}$$

on the weight of the GME component in any decomposition of ρ in Eq. (2) (equivalently, an upper bound on P_{BS}). It is easy to see that the minimal weight P_{GME} over all decomposition of a state ρ is a GME measure [54]: it is by definition nonzero for all GME states and zero for biseparable ones, it is convex, and it cannot increase under local operation with classical communication. Thus, the DDIC method allows us not only to certify GME, but also to quantify it, via Eq. (3). This quantification is both device-independent and scalable with the number of parties N.

Experimental results.—Our basic ingredient to prepare multipartite entangled states is a sandwichlike EPR source generating polarization-entangled photon pairs as shown in Fig. 2 [55]. Four-photon entangled states are prepared by entangling photons from two such EPR sources, i.e., by using postselection to project the initial state into the desired entangled state with a certain probability. In the experiment, we use two kinds of optical elements (the PBS and PDBS shown in Fig. 2) to realize different projectors and generate different families of four-photon or three-photon entangled states, including GHZ, cluster,

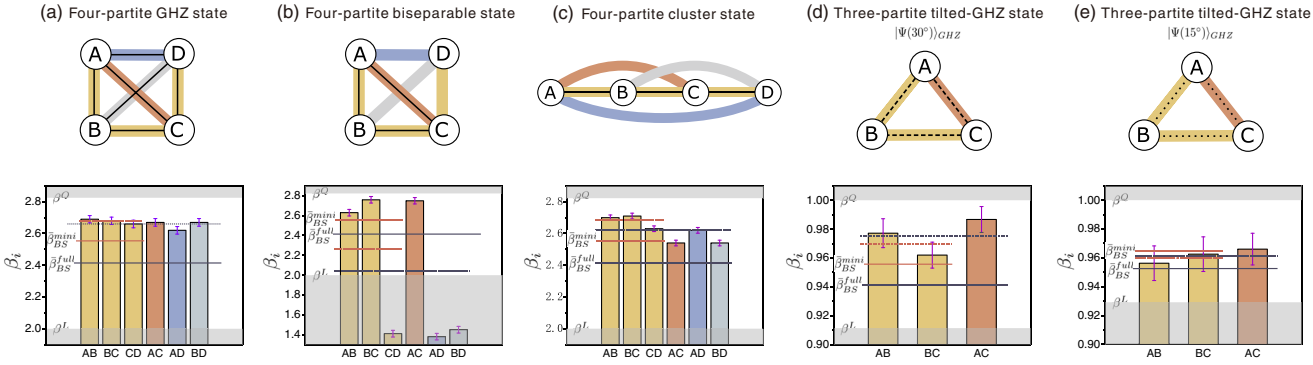

FIG. 3. DDIC results of several classes of entangled states. In (a)–(d), pictorial representations of four families of multipartite entangled states are diagrammed respectively for four-partite GHZ state, four-partite separable state, four-partite cluster state, and three-partite tilted GHZ states with different tilting angles. Each party is labeled as the circles, the thin solid edges give the graph-state representation of the state, while the thick colored edges give the pairs of parties for the DDIC method. The thick edges in yellow constitute a minimum covering in which all parties are connected, and the full covering consists of all edges. The histogram below each diagram represents the measured Bell value of each edge in minimum or full coverings. The brown and black dotted (solid) lines represent the mean Bell values (biseparable bounds) over the pairs in minimum or full coverings, respectively. The upper and lower shadow areas represent the quantum bound and local bound of the bipartite inequality.

and weighted graph states. For each family of states, we test the GME with the DDIC method described above.

Four-photon GHZ state.—The GHZ states $(1/\sqrt{2})\times(|0\rangle^{\otimes N}+|1\rangle^{\otimes N})$ are useful for many applications [56,57]. A four-photon GHZ state is represented as a tetrahedron in graph-state representation [58], consisting of four vertices (parties) and six edges (pairs). By projecting two parties into the Pauli X basis, the remaining two parties are prepared in the maximally entangled two-qubit states in all branches X^+X^+, X^+X^-, X^-X^+, X^-X^- (where $\pm$ represents the result of each X measurement). Interestingly, the states in the four branches are related by the action of a Pauli Z on one of the qubits, and hence can maximally violate the CHSH inequality with the same settings (upon classical relabeling). The CHSH value of each pair β_e $(e=AB,BC,CD,AC,AD,BD)$ is defined as the averaged violation of CHSH inequality over these branches. In the experiment, the four-photon GHZ state $|\Psi\rangle_{\mathrm{GHZ}}=(1/\sqrt{2})(|HHHH\rangle_{ABCD}+|VVVV\rangle_{ABCD})$ is prepared with the fidelity ~0.97, where H (V) denotes the horizontal (vertical) polarization of the photon. The CHSH values of all the six pairs are measured and shown in Fig. 3(a). To certify GME, the mean CHSH values over the pairs in the minimum and full coverings are calculated to be $\bar{\beta}^E=2.671\pm0.012$ and 2.662 ± 0.009, respectively, represented as dotted red or blue lines across the columns. It can be seen that the measured average CHSH values are well above the biseparable bound for the minimum and full coverings, computed to be 2.552 and 2.414. From the full covering we find that the prepared state has $P_{\mathrm{GME}}\geq 0.598\pm0.024$, after the filtering defined by postselection.

Biseparable state.—To see how to distinguish a biseparable state with our DDIC method, we prepare a four-photon state $|\Psi\rangle_{\mathrm{sep}}=\frac{1}{2}(|HHH\rangle_{ABC}+|VVV\rangle_{ABC})\otimes(|H\rangle_D+|V\rangle_D)$. The DIC implementation is analogous to the four-photon GHZ state; the measured results of all the six pairs are shown in Fig. 3(b). One sees that if a pair involves the isolated photon D, the measured CHSH value $\beta_{XD}(X=A,B,C)$ is below 2. The mean CHSH values for the minimum and full coverings are calculated to be 2.263 ± 0.020 and 2.067 ± 0.014, respectively, below the corresponding biseparable bounds. On the other hand, for the three-photon GHZ state prepared on parties ABC we find that $P_{\mathrm{GME}}\geq 0.785\pm0.035$. This shows that the state has entanglement depth 3 [59].

Cluster state.—The cluster states, e.g., $|\Psi\rangle_{\mathrm{cluster}}=\frac{1}{2}(|0000\rangle_{ABCD}+|0011\rangle_{ABCD}+|1100\rangle_{ABCD}-|1111\rangle_{ABCD})$, have been recognized as the basic building blocks for one-way quantum computation [60]. Cluster states are graph states with a lattice graph (with low degree); thus, a maximally entangled two-qubit state on an edge $e\in G$ (graph-state representation) can be prepared by only measuring the few neighboring parties. In the case of linear cluster states this requires one to measure only one or two parties. Hence, for the minimal covering at most four parties have to be measured in each run of the experiment, which is a great asset for scaling up N given that each measurement adds some noise to the state. In our four-photon experiment, this can be seen when measuring the pair AB (or CD), where only photon C (or B) need to be measured, and the last photon just acts as a trigger. The produced state is close to the linear cluster state $|\Psi\rangle_{\mathrm{cluster}}$ with fidelity ~0.95. The averaged CHSH values for the six pairs are shown in Fig. 3(c). The mean CHSH values for the minimum and full coverings are 2.653 ± 0.010 and 2.620 ± 0.007, respectively, which violate the biseparable bounds. The GME weight of cluster state is found to be $P_{\mathrm{GME}}\geq 0.497\pm0.017$.

Generalized GHZ state.—To illustrate the generality of the DDIC method we now apply it to several weakly entangled three-qubit states. In the experiment, we first prepare a tilted GHZ state $|\Psi(\theta)\rangle_{\mathrm{GHZ}} = \cos\theta|0\rangle^{\otimes 3} + \sin\theta|1\rangle^{\otimes 3}$ with $\theta = 30°$, the state fidelity is 96.4%. For this state, it is impossible to produce maximally entangled bipartite states on all branches. Instead with a Pauli X measurement on one of the qubits we prepare partially entangled states $\cos(\theta)|00\rangle \pm \sin(\theta)|11\rangle$. Thus, we choose the tilted CHSH inequality $\mathcal{I}_\theta$ [46] as the bipartite Bell inequality, which can be maximally violated by the state. Note that according to the Schmidt decomposition, it is enough to consider the tilted CHSH family of Bell inequalities for any entangled bipartite qubit state. We use the normalized Bell expression $\bar{\mathcal{I}}_{30°}$ for which we have $\beta^Q = 1$ and $\beta^L = 0.911$, and the biseparable bounds for minimum and full coverings are 0.956 and 0.941, respectively. The measured mean Bell values [Fig. 3(d)] are calculated to be 0.982 ± 0.006 and 0.975 ± 0.006 of minimum and full coverings, respectively, which clearly violate the biseparable bounds. Quantitatively, we find that $P_{\mathrm{GME}} \geq 0.582 \pm 0.082$. In the SM [48], we further illustrate the robustness to imperfections of the DDIC method by adding noise onto this state.

Finally, we prepare a more tilted GHZ state with $\theta = 15°$ and fidelity 98.7%. Numerical search shows the angle of the tilted inequality that is most robust to white noise is about 28°. The quantum and local bounds for $\bar{\mathcal{I}}_{28°}$ are $\beta^Q = 1$ and $\beta^L = 0.929$, respectively. The measured mean Bell value for the full covering is 0.962 ± 0.007, which is above the biseparable bound of $\bar{\beta}^{\mathrm{full}}_{\mathrm{BS}} = 0.953$, thus certifying GME of the state [Fig. 3(e)]. Note that the considered tilted GHZ state with $\theta \leq 15°$ cannot violate the standard Svetlichny inequality [61,62]. Demonstration of GME with a tripartite inequality would require a dedicated Svetlichny-type inequality [63]. Here, we are able to demonstrate GME by simply choosing adequate bipartite Bell inequality, demonstrating the flexibility of our method.

Discussion.—The DDIC method provides a way for reliable GME certification in a wide range of states. It also enables the quantification of genuine multipartite entanglement via the weight of the minimal GME component, and moreover is both device-independent and intrinsically resistant to realistic noise. This allows us to demonstrate and quantify GME experimentally in a variety of multipartite states, including in a genuinely but weakly entangled state. The DDIC method infers properties of multipartite states by leveraging bipartite Bell tests in an optimal way. When applied to generalized and weighted graph states with bounded degree, this allows the method to involve at most a constant number of parties in each run of the experiment.

This work was supported by the Innovation Program for Quantum Science and Technology (Grant No. 2021ZD0301604), National Natural Science Foundation of China (Grant No. 11874344, No. 61835004, No. 12122410, No. 92065107, No. 61327901, No. 11774335, No. 91536219, No. 11821404, No. 62075208, No. 62205326, No. 11734015), Anhui Initiative in Quantum Information Technologies (AHY020100, AHY060300), the Fundamental Research Funds for the Central Universities (Grant No. WK2030020019, No. WK2470000026, No. WK2030000038, No. WK2470000034, No. WK2030000061), China Postdoctoral Science Foundation (Grant No. 2020M682002). This work was partially carried out at the USTC Center for Micro and Nanoscale Research and Fabrication.

C. Z. and W.-H. Z contributed equally to this work.

*Corresponding author.
pavel.sekatski@gmail.com
†Corresponding author.
jdbancal.physics@gmail.com
‡Corresponding author.
michael.zwerger@mpl.mpg.de
§Corresponding author.
hyf@ustc.edu.cn
‖Corresponding author.
chengeng@ustc.edu.cn
¶Corresponding author.
cfli@ustc.edu.cn

[1] C. Song, K. Xu, H. Li *et al.*, Science **365**, 574 (2019).
[2] A. Omran, H. Levine, A. Keesling *et al.*, Science **365**, 570 (2019).
[3] O. Gühne and G. Tóth, Phys. Rep. **474**, 1 (2009).
[4] G. Tóth and O. Gühne, Phys. Rev. Lett. **94**, 060501 (2005).
[5] Y. Y. Zhao, G. Y. Xiang, X. M. Hu, B. H. Liu, C. F. Li, G. C. Guo, R. Schwonnek, and R. Wolf, Phys. Rev. Lett. **122**, 220401 (2019).
[6] Z. Hradil, Phys. Rev. A **55**, R1561(R) (1997).
[7] *Lecture Notes in Physics*, edited by M. Paris and J. Rehacek (Springer, Berlin, 2004), Vol. 649.
[8] Z. Hou, H. S. Zhong, Y. Tian, D. Dong, B. Qi, L Li, Y. Wang, F. Nori, G. Y. Xiang, C. F. Li, and G. C. Guo, New J. Phys. **18**, 083036 (2016).
[9] W. H. Zhang *et al.*, Phys. Rev. Lett. **125**, 030506 (2020).
[10] M. Hayashi, K. Matsumoto, and Y. Tsuda, J. Phys. A **39**, 14427 (2006).
[11] S. Pallister, N. Linden, and A. Montanaro, Phys. Rev. Lett. **120**, 170502 (2018).
[12] Z. Li, Y. G. Han, and H. Zhu, Phys. Rev. Appl. **13**, 054002 (2020).
[13] T. Moroder, O. Gühne, N. Beaudry, M. Piani, and N. Lutkenhaus, Phys. Rev. A **81**, 052342 (2010).
[14] D. Rosset, R. Ferretti-Schöbitz, J-D. Bancal, N. Gisin, and Y-C. Liang, Phys. Rev. A **86**, 062325 (2012).
[15] L. Lydersen, C. Wiechers, C. Wittmann, D. Elser, J. Skaar, and V. Makarov, Nat. Photonics **4**, 686 (2010).
[16] I. Gerhardt, Q. Liu, A. Lamas-Linares, J. Skaar, C. Kurtsiefer, and V. Makarov, Nat. Commun. **2**, 349 (2011).

[17] N. Brunner, D. Cavalcanti, S. Pironio, V. Scarani, and S. Wehner, Rev. Mod. Phys. **86**, 419 (2014).
[18] A. Acín, N. Brunner, N. Gisin, S. Massar, S. Pironio, and V. Scarani, Phys. Rev. Lett. **98**, 230501 (2007).
[19] A. Acín, N. Gisin, and L. Masanes, Phys. Rev. Lett. **97**, 120405 (2006).
[20] L. Masanes, S. Pironio, and A. Acín, Nat. Commun. **2**, 238 (2011).
[21] S. Pironio, A. Acín, S. Massar, A. Boyer de la Giroday, D. N. Matsukevich, P. Maunz, S. Olmschenk, D. Hayes, L. Luo, T. A. Manning, and C. Monroe, Nature (London) **464**, 1021 (2010).
[22] T. Lunghi, J. B. Brask, Charles Ci Wen Lim, Q. Lavigne, J. Bowles, A. Martin, H. Zbinden, and N. Brunner, Phys. Rev. Lett. **114**, 150501 (2015).
[23] K. F. Pál, T. Vértesi, and M. Navascués, Phys. Rev. A **90**, 042340 (2014).
[24] S. L. Chen, C. Budroni, Y. C. Liang, and Y. N. Chen, Phys. Rev. Lett. **116**, 242401 (2016).
[25] R. Rabelo, Y. Z. Law, and V. Scarani, Phys. Rev. Lett. **109**, 180401 (2012).
[26] R. Rabelo, M. Ho, D. Cavalcanti, N. Brunner, and V. Scarani, Phys. Rev. Lett. **107**, 050502 (2011).
[27] N. Gisin, Phys. Lett. A **154**, 201 (1991).
[28] N. Gisin and A. Peres, Phys. Lett. A **162**, 15 (1992).
[29] J. Bell, Physics **1**, 195 (1964).
[30] S. Popescu and D. Rohrlich, Phys. Lett. A **169**, 411 (1992).
[31] S. Popescu and D. Rohrlich, Phys. Lett. A **166**, 293 (1992).
[32] M. Gachechiladze and O. Gühne, Phys. Lett. A **381**, 1281 (2017).
[33] S. K. Choudhary, S. Ghosh, G. Kar, and R. Rahaman, Phys. Rev. A **81**, 042107 (2010).
[34] M. Li and S.-M. Fei, Phys. Rev. Lett. **104**, 240502 (2010).
[35] J.-D. Bancal, N. Brunner, N. Gisin, and Y.-C. Liang, Phys. Rev. Lett. **106**, 020405 (2011).
[36] J.-D. Bancal, N. Gisin, Y.-C. Liang, and S. Pironio, Phys. Rev. Lett. **106**, 250404 (2011).
[37] Y.-C. Liang, D. Rosset, J.-D. Bancal, G. Putz, T. J. Barnea, and N. Gisin, Phys. Rev. Lett. **114**, 190401 (2015).
[38] M.-X. Luo, Phys. Rev. A **98**, 042317 (2018).
[39] I. Šupić and J. Bowles, Quantum **4**, 337 (2020).
[40] J. Kaniewski, Phys. Rev. Lett. **117**, 070402 (2016).
[41] A. Coladangelo, K. T. Goh, and V. Scarani, Nat. Commun. **8**, 15485 (2017).
[42] W. H. Zhang, G. Chen, X. X. Peng, X. J. Ye, P. Yin, Y. Xiao, Z. B. Hou, Z. D. Cheng, Y. C. Wu, J. S. Xu, C. F. Li, and G. C. Guo, Phys. Rev. Lett. **121**, 240402 (2018).
[43] W. H. Zhang *et al.*, npj Quantum Inf. **5**, 4 (2019).
[44] F. Baccari, R. Augusiak, I. Šupić, J. Tura, and A. Acín, Phys. Rev. Lett. **124**, 020402 (2020).
[45] M. Zwerger, W. Dür, J.-D. Bancal, and P. Sekatski, Phys. Rev. Lett. **122**, 060502 (2019).
[46] A. Acín, S. Massar, and S. Pironio, Phys. Rev. Lett. **108**, 100402 (2012).
[47] D. Orsucci, J.-D. Bancal, N. Sangouard, and P. Sekatski, Quantum **4**, 238 (2020).
[48] See Supplemental Material, which includes Refs. [49–52], at http://link.aps.org/supplemental/10.1103/PhysRevLett.129.190503; for a detailed discussion of postselection under weak-fair sampling assumption, an outline of the DDIC protocol, a discussion on the implications of the choice of the covering on the biseparable bound, the proof of optimality of the ring covering, a detailed description of the experiment, and a discussion on the robustness of the DDIC method.
[49] D. W. Berry, H. Jeong, M. Stobinska, and T. C. Ralph, Phys. Rev. A **81**, 012109 (2010).
[50] J.-W. Pan, Z.-B. Chen, C.-Y. Lu, H. Weinfurter, A. Zeilinger, and M. Zukowski, Rev. Mod. Phys. **84**, 777 (2012).
[51] N. Kiesel, C. Schmid, U. Weber, G. Toth, O. Guhne, R. Ursin, and H. Weinfurter, Phys. Rev. Lett. **95**, 210502 (2005).
[52] C. Zhang, Y.-F. Huang, B.-H. Liu, C.-F. Li, and G.-C. Guo, Phys. Rev. A **93**, 062329 (2016).
[53] In general, a sequence of local operation with classical communication (LOCC) may be performed on the remaining particles R
[54] Z. H. Ma, Z. H. Chen, J. L. Chen, C. Spengler, A. Gabriel, and M. Huber, Phys. Rev. A **83**, 062325 (2011).
[55] C. Zhang, Y.-F. Huang, Z. Wang, B.-H. Liu, C.-F. Li, and G.-C. Guo, Phys. Rev. Lett. **115**, 260402 (2015).
[56] Zhi Zhao, Yu-Ao Chen, An-Ning Zhang, Tao Yang, Hans J. Briegel, and Jian-Wei Pan, Nature (London) **430**, 54 (2004).
[57] J. Kempe, Phys. Rev. A **60**, 910 (1999).
[58] M. Hein, W. Dür, J. Eisert, R. Raussendorf, M. Van den Nest, and H.-J. Briegel, arXiv:quant-ph/0602096.
[59] A. S. Sørensen and K. Mølmer, Phys. Rev. Lett. **86**, 4431 (2001).
[60] P. Walther, K. J. Resch, T. Rudolph, E. Schenck, H. Weinfurter, V. Vedral, M. Aspelmeyer, and A. Zeilinger, Nature (London) **434**, 169 (2005).
[61] G. Svetlichny, Phys. Rev. D **35**, 3066 (1987).
[62] M. Zukowski, C. Brukner, W. Laskowski, and M. Wiesniak, Phys. Rev. Lett. **88**, 210402 (2002).
[63] J-D. Bancal, N. Gisin, and P. J. Pironio, J. Phys. A **43**, 385303 (2010).